Electronic supplementary information

An Ultralow-Concentration (0.05 M) Electrolyte for Advanced K-Ion Batteries

Guo-Yu Zhu[#[a]], Guo-Zhan Yang[#[a]], Bai-Hua Huang[[a]], Bo Wang[[a]], Xue-Bing Ye[[a]], Ze-Lin Zheng [[a]], Bao-Qi Feng[[a]], Xian Zeng[[a]], De-Shan Bin*[[a]], Lin Liu* [[b]], and Dan Li[[a]]

Experimental Section

Electrolytes

Electrolytes were potassium bis (fluorosulfonyl) imide (KFSI) dissolved into the solvents of EC: EMC (1:1, volume ratio) at concentrations of 0.025 M, 0.05 M, and 1.0 M.

Materials synthesis

The ASHCs samples were prepared by mixing 3S-AFs with sublime sulfur (1:3, mass ratio), and then pyrolyzed at 450 ℃ for 5 h under argon flow.[1, 2] The hard carbon samples were prepared by 1S-AFs, which were pyrolyzed at 1200 ℃ for 2 h under argon flow.[1] The soft carbon samples were prepared by pitch, which were pyrolyzed at 800 ℃ for 2 h under argon flow.

Characterization Methods

Viscosity and density were tested by falling sphere viscosimeter (Lovis 2000 M). Electric conductivity was tested via conductivity meter (HZPD-T503). Powder X-ray diffraction (PXRD) pattern was tested at miniflex600 X-Ray diffractometer (Rigaku) using Cu Kα irradiation. TEM was acquired with a JEOL JEM-2100F instrument. SEM images were acquired on Hitachi FlexSEM1000 II. X-ray photoelectron spectroscopy (XPS) data were measured by a Thermo Scientific K-Alpha+. Raman spectra was performed at HORIBA LabRAM HR Evolution (λ= 532 nm).

Electrochemical measurements

The ASHCs anode was prepared by mixing the active materials, super P and binder of sodium carboxymethyl cellulose/styrene-butadiene rubber (CMC/SBR) or poly (vinylidene fluoride) (PVDF) at a weight ratio of 7:2:1. Then the slurry was pasted onto Cu foil. The HC and SC anodes were prepared by casting the slurry of active materials, super P, and CMC/SBR at weight ratio of 8:1:1 onto Cu foil. Then, these slurries were dried under vacuum conditions at 60°C for 12 hours. The mass loading of active materials of electrodes was about 0.9–1.3 mg cm^{-2}. The assembly process was conducted within an argon-filled glovebox, maintaining oxygen and water below 0.1 ppm. During the assembly of R2032-type coin cells, glass microfiber filter (Whatman) was used as the separator and potassium metal (Sigma Ltd) was functioned as the counter electrode. Galvanostatic charge–discharge tests with a voltage window of 0.01–3.0 V were tested by a Neware Battery Testing system at 25 ℃. At 0 ℃ and 60 ℃, the galvanostatic charge–discharge tests were tested by the LAND Battery Testing system. Cyclic voltammetry (CV) and Linear sweep voltammetry (LSV) were conducted on an electrochemical workstation (Metrohm Autolab). The galvanostatic intermittent titration technique (GITT) was employed to compare the diffusion coefficient of K^+ and over-potential of ASHCs anode with 0.05 M and 1.0 M electrolytes during the potassiation/depotassiation processes with a pulse current at 0.1 C via LAND Battery Testing system.

The CV tests with various scan rates were used to analyze the contribution of diffusion and capacitance. The relationship of peak current (i) and the scan rate (v) was expressed by Equation (1) and Equation (2):[3]

$$i = av^b \#(1)$$

$$\log i = b \log v + \log a \#(2)$$

Moreover, to quantify the contribution of diffusion and capacitance, Equation (3) is introduced:

$$i(v) = k_1 v + k_2 v^{\frac{1}{2}} \#(3)$$

Equation (3) could also be written as Equation (4):

$$i(v)/v^{\frac{1}{2}} = k_1 v^{\frac{1}{2}} + k_2 \#(4)$$

In Equation (3), v is the scan rates, k_1 and k_2 were constants. $k_1 v$ and $k_2 v^{1/2}$ reflected as the capacitive-controlled contribution and diffusion-controlled contribution, respectively. Based on Equation (4), we were able to determine

the value of k_1 and calculated the capacitive and diffusion contribution.

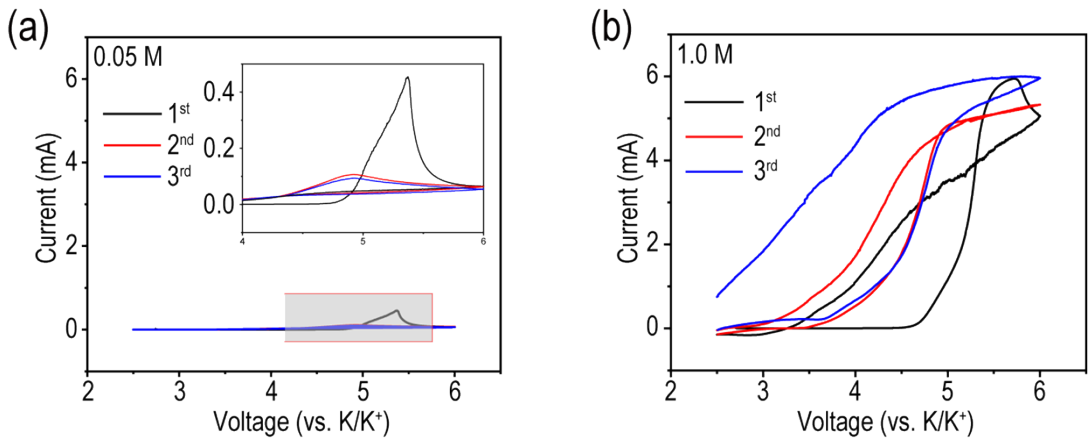

Fig. S1. Corrosion currents in 0.05 M and 1.0 M electrolytes on aluminum foil. (a) 0.05 M electrolyte. (b) 1.0 M electrolyte. CV tests of 0.05 M and 1.0 M electrolytes at a scanning rate of 0.1 mV s^{-1} in voltage ranges of 2.5–6.0 V in K||Al cells.

,

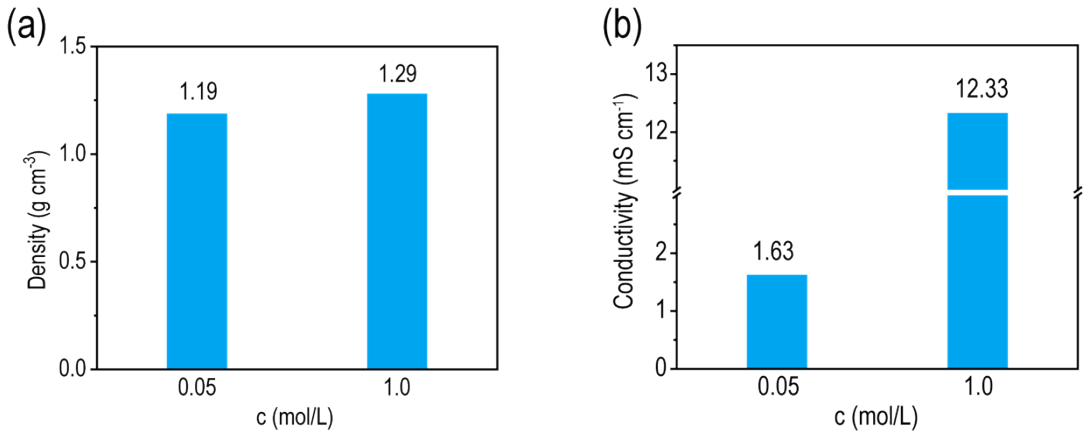

Fig. S2. Density and conductivity in 0.05 M and 1.0 M electrolytes. (a) Densities of 0.05 M and 1.0 M electrolytes. (b) Conductivities of 0.05 M and 1.0 M electrolytes.

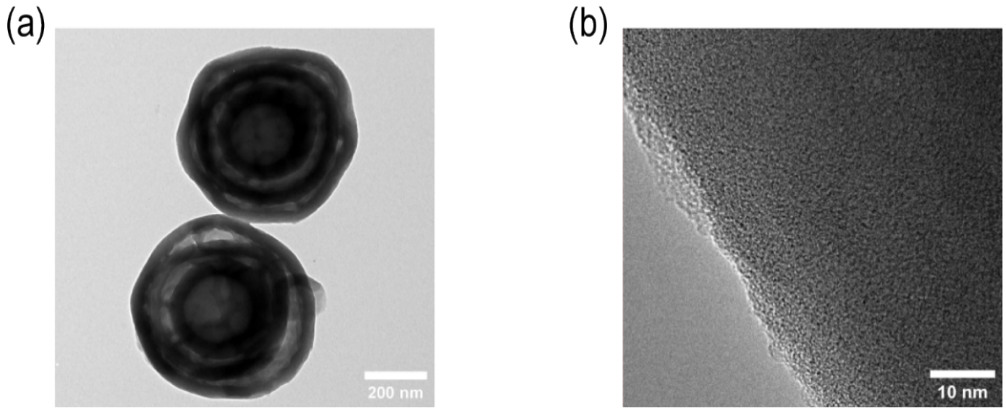

Fig. S3. Characterizations of ASHCs. (a) TEM image. (b) HRTEM image of edge.

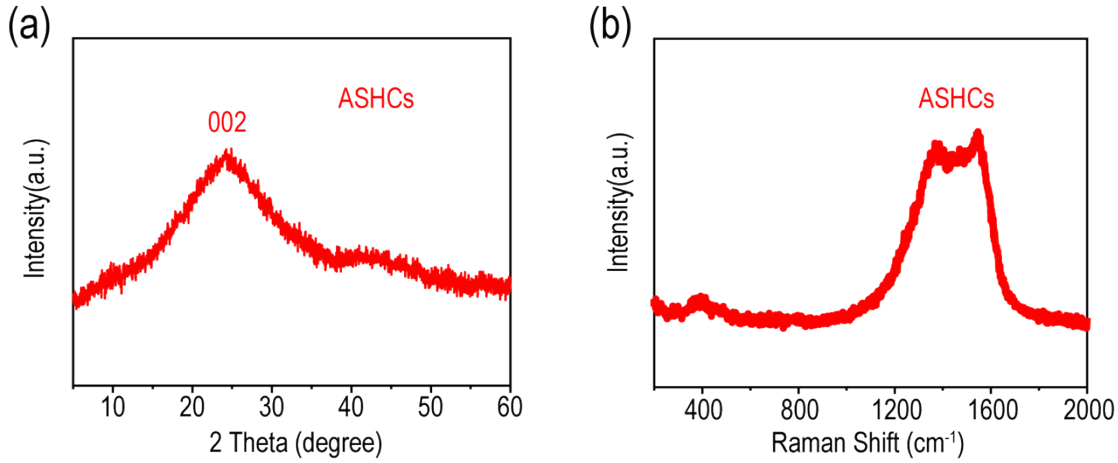

Fig. S4. Structural characterizations of ASHCs. (a) XRD pattern. (b) Raman spectrum.

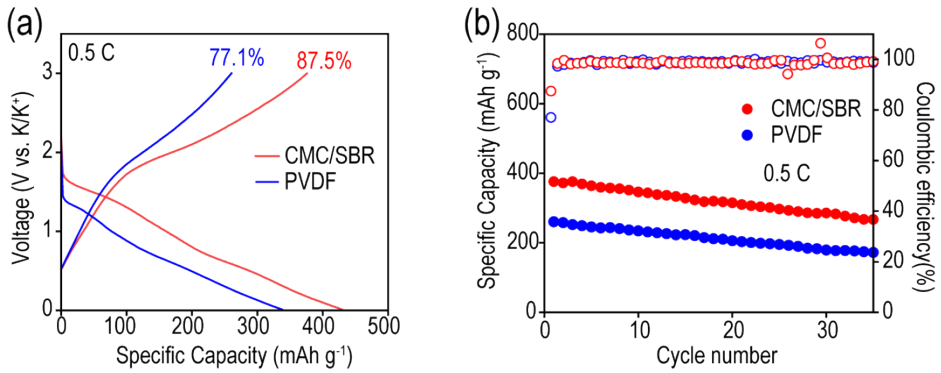

Fig. S5. The battery performance of ASHCs anode in 0.05 M electrolyte with PVDF and CMC/SBR as binders. (a) The typical charge/discharge profiles at 0.5 C. (b) 0.5 C for 35 cycles.

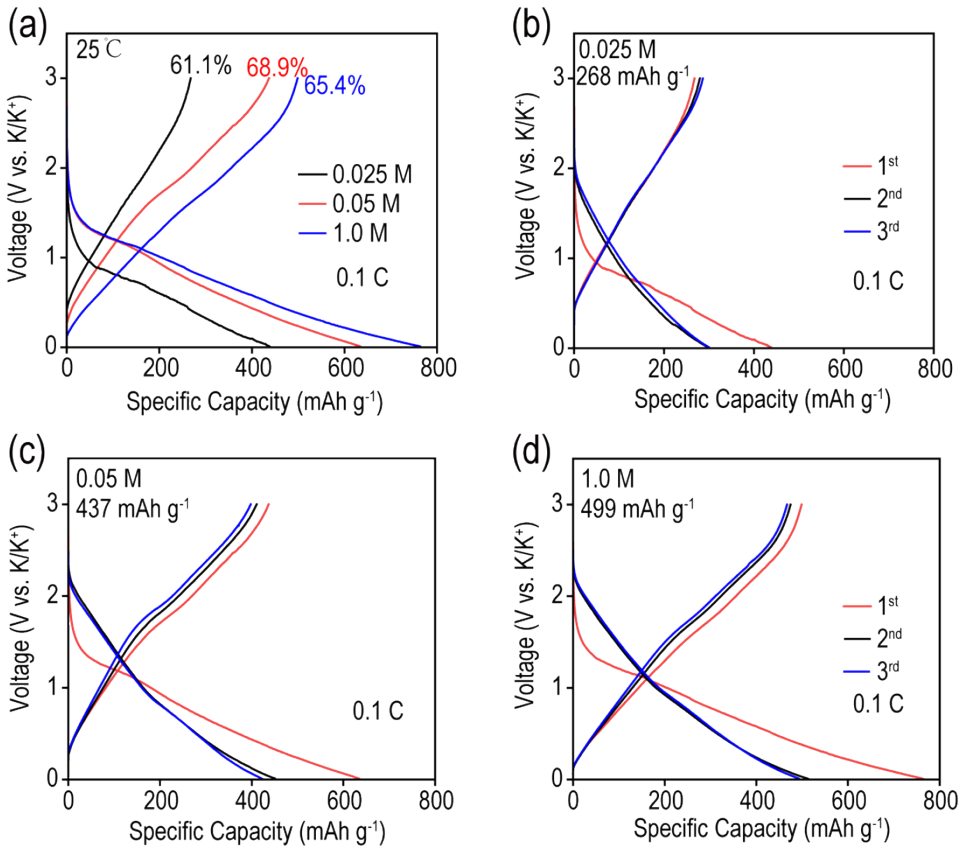

Fig. S6. (a) The charge/discharge profiles for the first cycle with different concentration electrolytes at 0.1 C at 25 ℃. The first third charge-discharge profiles in ASHCs anode used different concentration electrolytes. (b) 0.025 M; (b) 0.05 M; (c) 1.0 M.

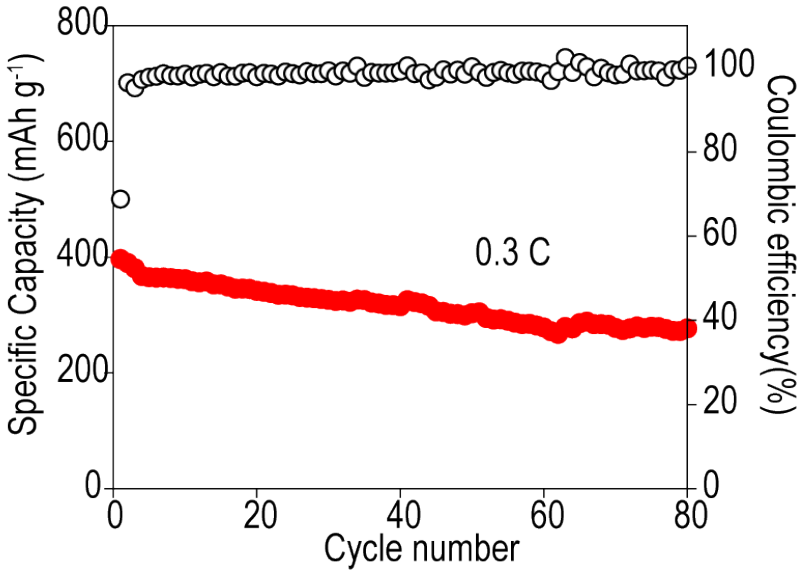

Fig. S7. Cyclability of the ASHCs anode in the 0.05 M electrolyte for 80 cycles at 0.3 C.

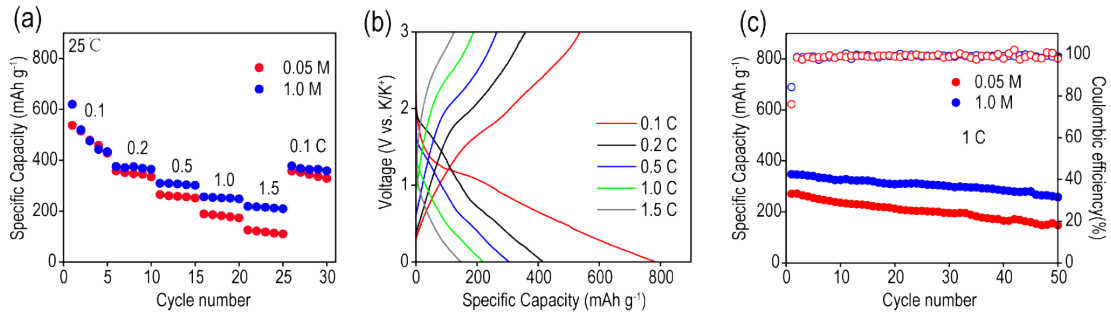

Fig. S8. (a) Rate performance of the ASHCs anode in 0.05 M and 1.0 M electrolytes at 25 ℃. (b) Charge–discharge profiles various current densities of 0.05 M electrolyte. (c) Cycling capacity in 0.05 M and 1.0 M electrolytes at 1 C for 50 cycles after 5 cycles at 0.2 C.

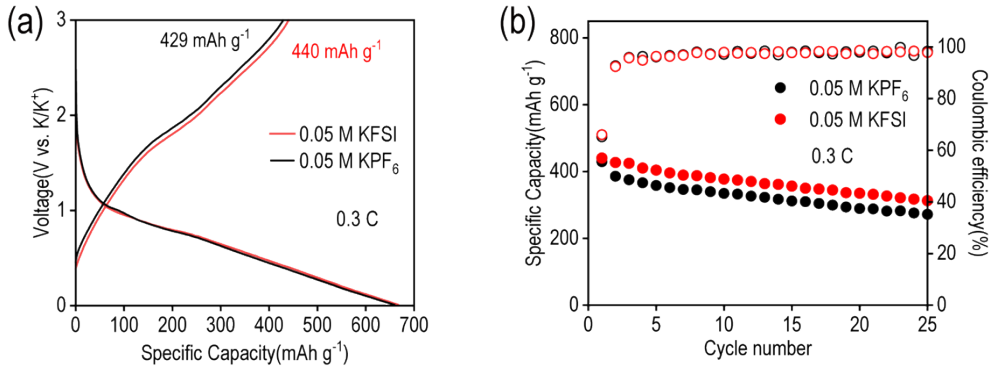

Fig. S9. Electrochemical performance of the ASHCs anode in 0.05 M KFSI and 0.05 M KPF_6 electrolytes in half-cell KIBs. (a) The typical charge/discharge profiles at 0.3 C. (b) Cycling capacity at 0.3 C for 25 cycles.

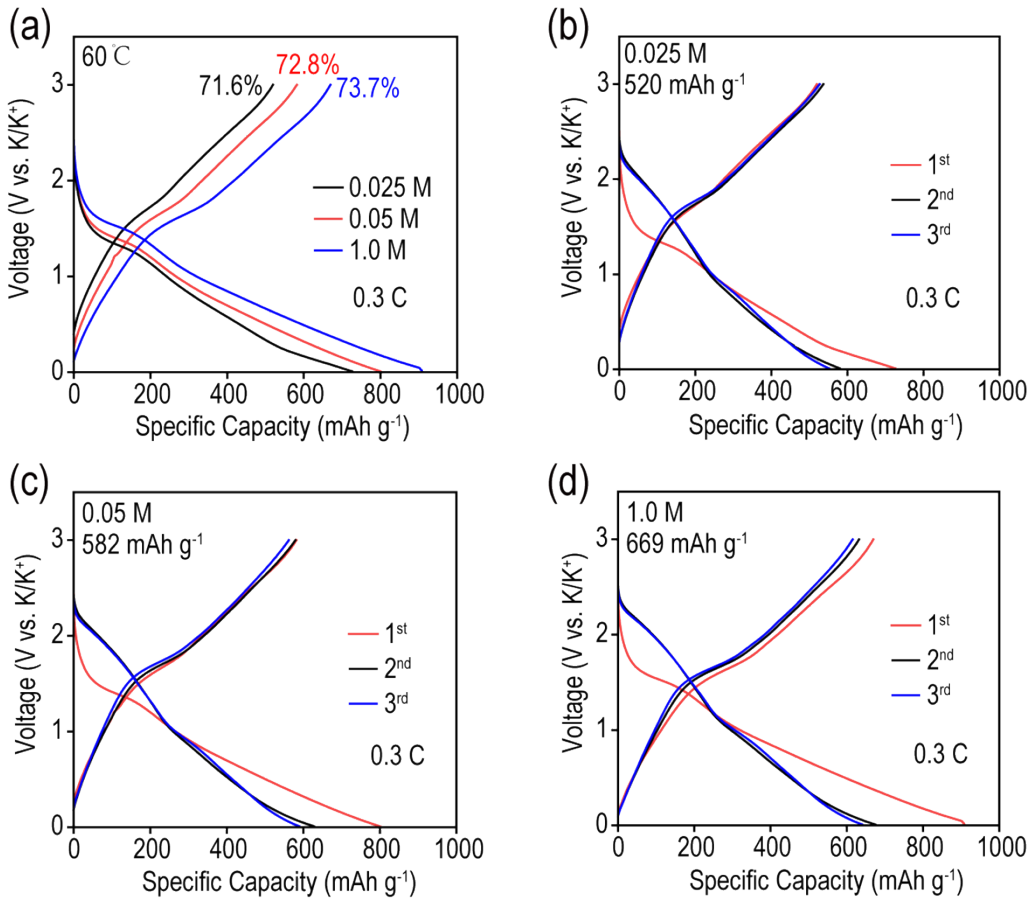

Fig. S10. (a) The charge/discharge profiles for the first cycle with different concentration electrolytes at 0.3 C at 60 ℃. The first third charge-discharge curves in ASHCs anode used different concentration electrolytes. (b) 0.025 M; (b) 0.05 M; (c) 1.0 M.

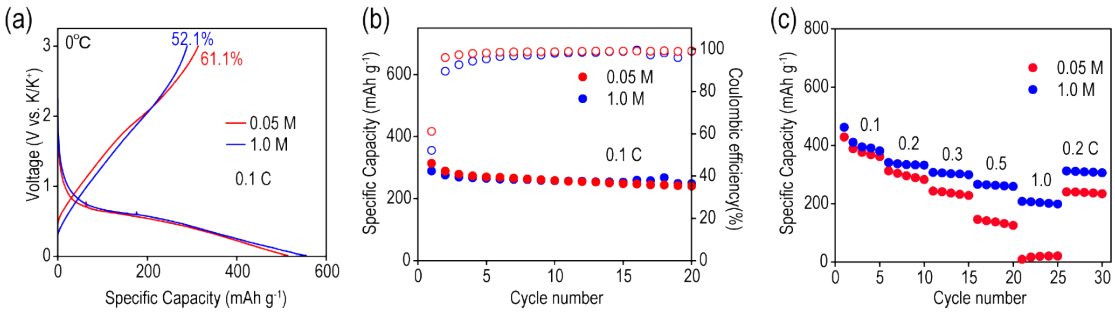

Fig. S11. Electrochemical performance of the ASHCs anode in 0.05 M and 1.0 M electrolytes at 0 ℃ in half-cell KIBs. (a) The typical charge/discharge profiles at 0.1 C. (b) Cycling capacity at 0.1 C for 20 cycles. (c) Rate performance of the ASHCs anode in 0.05 M and 1.0 M electrolytes at 0 ℃.

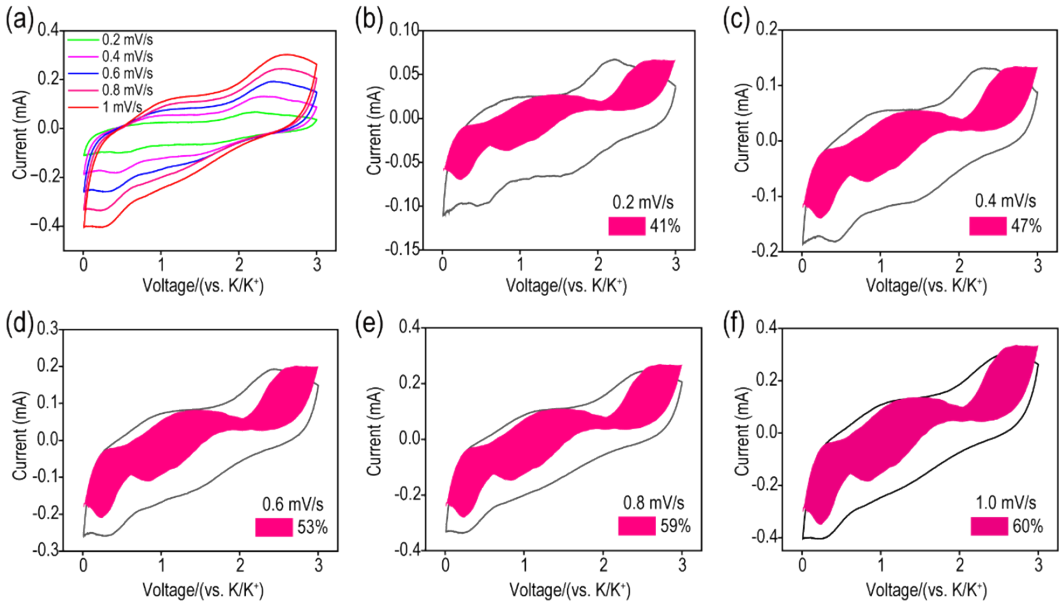

Fig. S12. (a) CV curves of 0.05 M electrolyte at 0.2-1.0 mV s^{-1}. (b-f) Contribution of capacitance process at various scan rates: (b) 0.2 mV s^{-1}; (c) 0.4 mV s^{-1}; (d) 0.6 mV s^{-1}; (e) 0.8 mV s^{-1}; (f) 1.0 mV s^{-1}.

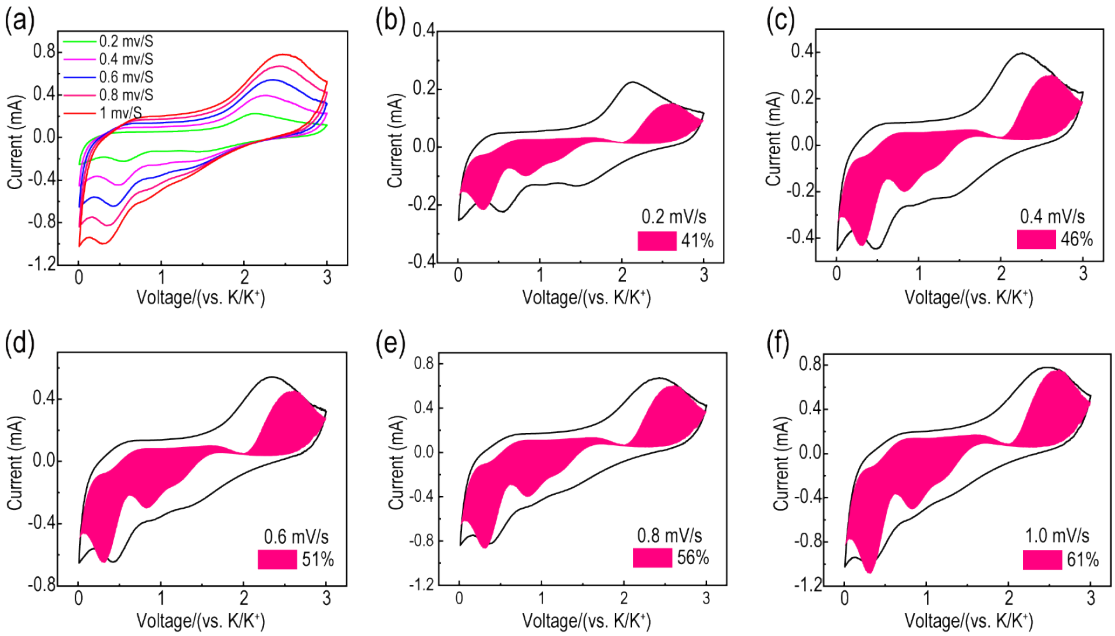

Fig. S13. (a) CV curves of 1.0 M electrolyte at 0.2-1.0 mV s^{-1}. (b-f) Contribution of capacitance process at various scan rates: (b) 0.2 mV s^{-1}; (c) 0.4 mV s^{-1}; (d) 0.6 mV s^{-1}; (e) 0.8 mV s^{-1}; (f) 1.0 mV s^{-1}.

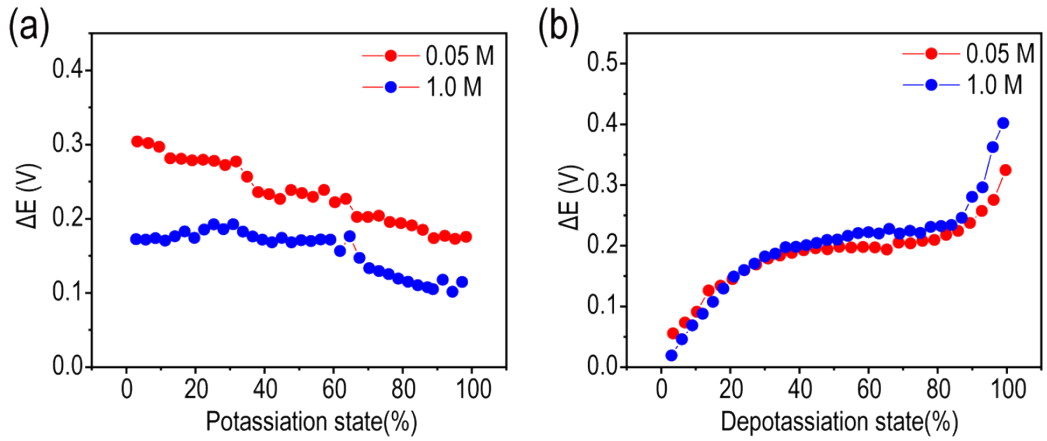

Fig. S14. Overpotential with 0.05 M and 1.0 M electrolytes during a) potassiation and b) depotassiation processes.

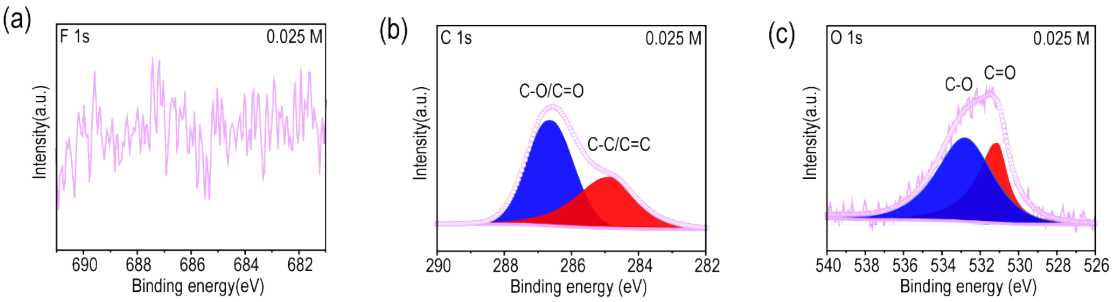

Fig. S15. The F 1s, C 1s and O 1s high-resolution XPS spectra of ASHCs anode in a–c) the 0.025 M electrolyte after 50 cycles.

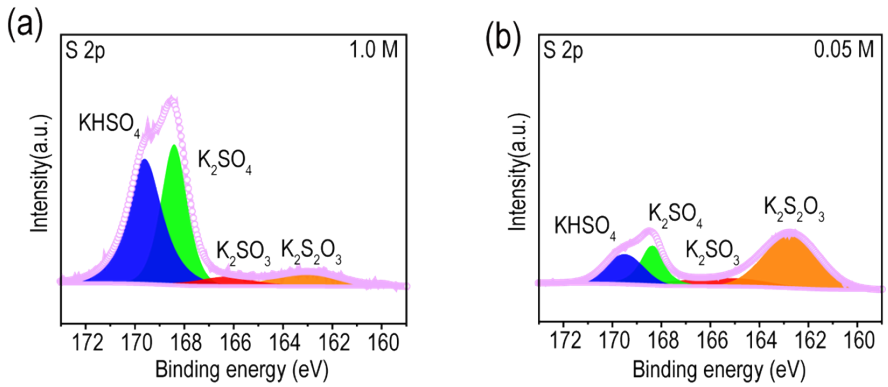

Fig. S16 The S 2p high-resolution XPS spectra of ASHCs anode after 50 cycles in the 1.0 M electrolyte (a) and 0.05 M electrolyte (b).

Table S1. The percent composition of elements in SEI.

	C	O	K	S	F	N
1.0 M	50.3%	22.7%	19.3%	3.1%	2.8%	1.8%
0.05 M	54.4%	21.9%	18.7%	2.0%	1.6%	1.4%
0.025 M	84.7%	7.0%	6.0%	0.3%	1.1%	0.9%

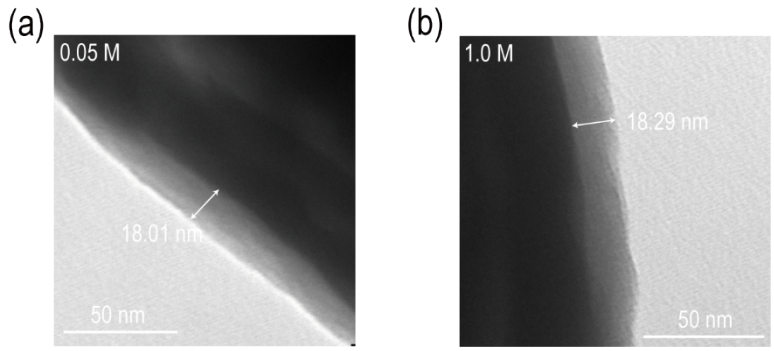

Fig. S17 The TEM image of the cycled ASHCs anodes of 0.05 M electrolyte (a) and 1.0 M electrolyte (b).

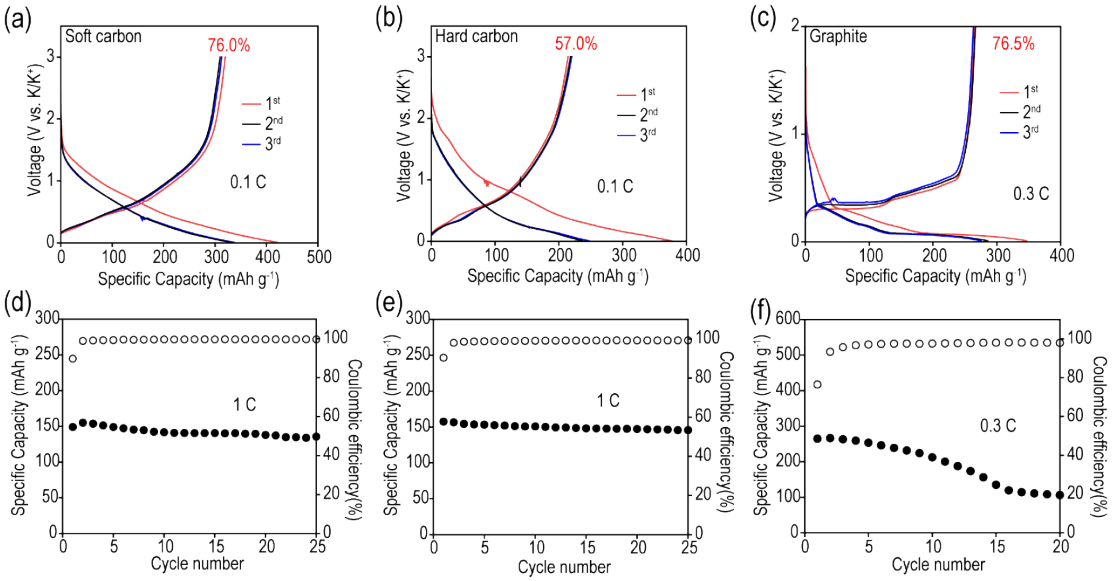

Fig. S18. Electrochemical performance of the soft carbon, hard carbon and graphite anodes with 0.05 M electrolyte in half-cell KIBs at 60 ℃. (a-c) Charge-discharge profiles in the first three cycles of soft carbon at 0.1 C (a), hard carbon at 0.1 C (b) and graphite anodes at 0.3 C (c). (d-e) Cycling capacity of soft carbon (d) and hard carbon anodes (e) for 25 cycles after 3 cycles at 0.1 C. (f) Cycling capacity of graphite anode for 20 cycles at 0.3 C.

1 D. S. Bin, Z. X. Chi, Y. T. Li, K. Zhang, X. Z. Yang, Y. G. Sun, J. Y. Piao, A. M. Cao and L. J. Wan, *J. Am. Chem. Soc.,* 2017, **139**, 13492-13498.

2 G. Z. Yang, Y. F Chen, B. Q. Feng, C. X. Ye, X. B. Ye, H. Jin, E. Zhou, X. Zeng, Z. L. Zheng, X. L. Chen, D. S. Bin and A. M. Cao, *Energy Environ. Sci.*, 2023, **16**, 1540-1547.

3 N. Sun, Z. Guan, Y. Liu, Y. Cao, Q. Zhu, H. Liu, Z. Wang, P. Zhang and B. Xu, *Adv. Energy Mater.,* 2019, **9**, 1901351.